IL NUOVO CIMENTO **46 C** (2023) 65
DOI 10.1393/ncc/i2023-23065-2

COMMUNICATIONS: SIF Congress 2022

The upgrade of the Pierre Auger Observatory: AugerPrime

G. A. ANASTASI([1])(*) for the PIERRE AUGER COLLABORATION([2])(**)(***)

([1]) *INFN, Sezione di Torino and Osservatorio Astrofisico di Torino (INAF) - Torino, Italy*
([2]) *Observatorio Pierre Auger - Av. San Martín Norte 304, 5613 Malargüe, Argentina*

received 31 January 2023

Summary. — Over the last 15 years the Pierre Auger Observatory has accumulated the world's largest exposure to ultrahigh-energy cosmic rays (UHECRs) and the analysis of this dataset led to major advances in our understanding of the nature of UHECRs. The new perspectives opened by the current results call for an upgrade of the Observatory (dubbed AugerPrime), whose main aim is the collection of new information about the primary mass of UHECRs, mandatory to interpret all the observations into a unified picture. The upgrade program includes: the installation of a plastic scintillator detector on top of each water-Cherenkov detector (WCD) of the surface array; the addition of a small photomultiplier tube in each WCD to extend the dynamic range of measurement; an array of underground scintillator detectors to measure the muonic component of extensive air showers; the deployment of a radio antenna atop each WCD; and new electronics to process the signals from all the detectors. An overview of the upgrade is provided, together with the expected performances and the improved physics sensitivity.

1. – Introduction

The Pierre Auger Observatory [1], located near the town of Malargüe (Mendoza, Argentina), is the largest experiment built for the study of ultrahigh-energy cosmic rays (UHECRs), namely astroparticles reaching the Earth with energies $\gtrsim 10^{17}$ eV. The Observatory was designed as a hybrid detector and comprises: an array of 1600 water-Cherenkov detectors (WCDs) arranged in a 1.5 km triangular grid over an area of $\sim$3000 km^2 (Surface Detector, SD); 24 fluorescence telescopes overlooking the SD with elevation angle $\approx 2°$–$30°$ from four buildings located at the edges of the array (Fluorescence Detector, FD).

(*) E-mail: ganastas@to.infn.it
(**) E-mail: spokespersons@auger.org
(***) Full author list: https://www.auger.org/archive/authors_2022_09.html

The UHECRs cannot be directly detected because of their very low flux, thus the cascades of secondary particles (known as extensive air showers, EAS) generated in the interaction of the primary cosmic rays with the atmosphere molecules are instead observed. The two systems, employing different detection techniques, provide a sampling measurement of the shower particles at ground level while simultaneously observing the fluorescence light emitted during their propagation in the atmosphere. Furthermore, the set of hybrid events allows a data-driven calibration while granting a thorough way of determining the systematic uncertainties of both components.

During the ∼18 years-long lifetime of the experiment, two denser arrays of water-Cherenkov stations with spacing 750 m and 433 m have been added to extend the measurements towards lower energies, together with 3 fluorescence telescopes overlooking the area with elevation from 30° to 60° (High Elevation Auger Telescopes, HEAT). Moreover, engineering arrays of underground muon detectors (Auger Muon and Infill for the Ground Array project, AMIGA) and radio antennas (Auger Engineering Radio Array, AERA) have also been installed in the same area.

Taking data continuously since the beginning of operations in 2004, the Pierre Auger Observatory has accumulated the world's largest exposure to UHECRs, leading to major contributions in understanding the nature of very energetic astroparticles, such as:

i) the unambiguous observation of the features in the energy spectrum, in particular the suppression of the flux starting around 40 EeV [2, 3];

ii) the study of the evolution of the mass composition below the flux suppression, which points toward an increase of the fraction of heavier primaries with energy [4, 5];

iii) the observation of a large-scale dipolar anisotropy in cosmic rays of energy above 8 EeV with significance $> 6\sigma$, which proves their extragalactic origin [6, 7];

iv) strong hints of correlation with starburst galaxies and Active Galactic Nuclei in intermediate-scale anisotropy searches for UHECR with $E \gtrsim 40$ EeV [8, 9].

In order to make further progress, the Pierre Auger Collaboration decided for an upgrade of the Observatory, dubbed AugerPrime [10,11], whose main aim is the collection of new observables sensitive to the mass of primary UHECRs. Indeed, determining the composition over the whole UHE range is the key to interpret all the measurements in a unified picture, but the hybrid event statistics is insufficient to reach this goal above $\sim 10^{19.5}$ eV due to the reduced duty cycle (∼15%) of the fluorescence telescopes, that can operate only in clear, moonless nights.

Based on the perspectives opened by the current findings, the upgrade will allow to:

- understand the origin of the flux suppression and constrain the characteristics of the possible sources;

- accomplish composition-driven anisotropy analyses and assess the feasibility of charged particle astronomy at the highest energies after evaluating the fraction of protons in the flux suppression region;

- allow for enhanced searches for UHE neutrino and γ-ray fluxes while investigating the potential for future experiments;

- study hadronic interactions in energy and kinematic regions not accessible to accelerators, to improve the existing models and, in particular, to address the inconsistencies in the muon content predicted by simulations with respect to data (the so-called muon-puzzle; see for example ref. [12]);
- search for non-standard physical processes, such as Lorentz invariance violation or super-heavy dark matter.

2. – AugerPrime design

The AugerPrime upgrade mainly consists of several new detectors added to the stations of the surface array (see fig. 1). A station consists of a 3.6 m diameter $\times$ 1.2 m height polyethylene tank containing 12000 liters of ultra-pure water inside a sealed liner with a reflective inner surface. The Cherenkov light produced by the passage of relativistic charged particles through the water is collected by three 9-inch Photonis XP1805 photomultiplier tubes (PMTs) located symmetrically at a distance of 1.20 m from the tank center. For the upgrade, a plastic scintillator (Scintillator Surface Detector, SSD) and a radio antenna (Radio Detector, RD) are placed on top of the water-Cherenkov tank, while an additional 1-inch diameter photomultiplier (Small PMT, SPMT) is installed inside the WCD. Moreover, an Underground Muon Detector (UMD) is deployed aside each WCD in the Infill area. An upgraded electronics (Upgraded Unified Board, UUB) has been devised to process the signals collected by all the detectors with improved performances and data processing capabilities.

The added components use the existing communication system of the station. The powering infrastructure remains unchanged too, except for the substitution of the solar panels to increase the power budget. Furthermore, the monitoring, data acquisition and

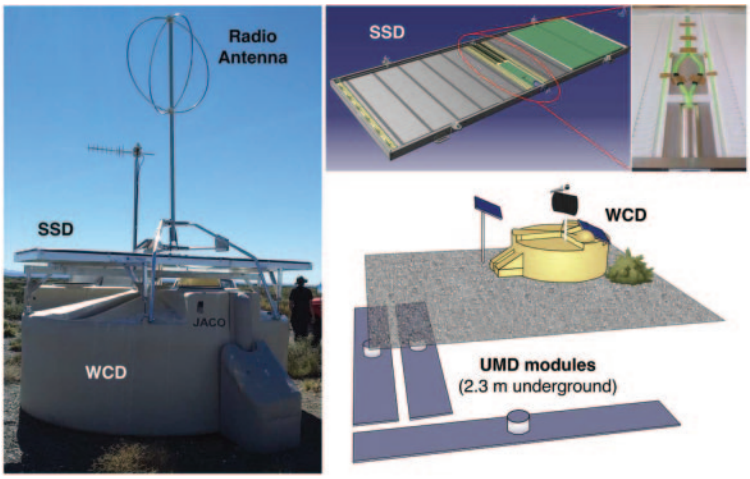

Fig. 1. – Left: an upgraded surface detector station, comprising a Water-Cherenkov Detector (WCD), a Scintillator Surface Detector (SSD) and a radio antenna. Photo from ref. [13]. Top right: rendering of a SSD module. The optical fibers are bundled to be coupled to the photomultiplier, as shown in the rigthmost picture. Images from ref. [14]. Bottom right: Schematic of an UMD position, comprising three 10 m^2 modules buried 2.3 m deep underground aside the station. Image from ref. [15].

reconstruction pipelines are being updated for AugerPrime, including the RD and UMD integration in the data-taking scheme. The data are continuously analysed to assess the conformity of the new detectors to the design requirements.

The upgraded station is designed to efficiently disentangle the electromagnetic and muonic components of an extensive air shower, allowing not only the reconstruction of the primary-particle energy but also of the depth of maximum of longitudinal development $X_{\rm max}$ and of the number of muons (two quantities which scale with the primary mass) on an event-by-event basis. Such results will be reached by means of multivariate analyses based on universality properties of the showers or exploiting the power of newly developed machine-learning techniques, and will provide unprecedented sensitivity to the mass composition of cosmic rays with extreme energies.

In the following, the design of the new detectors is presented.

2˙1. *The Scintillator Surface Detector (SSD).* – An SSD unit consists of a box of 3.8 m × 1.3 m containing two panels, each composed of 24 extruded polystyrene scintillator bars (1.6 m × 5 cm × 1 cm). The scintillators are housed in a light-tight, waterproof enclosure mounted on top of the WCDs with a strong support frame, designed to withstand strong winds. The scintillation light is collected by wavelength-shifting fibers inserted into two straight extruded holes in the scintillator bars. Such fibers are bundled and optically coupled to a single 1.5-inch photomultiplier tube (bi-alkali Hamamatsu R9420), with a power supply manufactured by the ISEG company according to a custom-made design.

The production and assembly of the SSD units is completed and all the detectors have been individually tested with atmospheric muons to check the light tightness and the response to minimum-ionizing particles (MIP). The uniformity of the measured signal was found equal to ±5% along one scintillator bar and ±10% between bars, with a value of (30 ± 2) photoelectrons per vertical MIP [14]. Also all the SSD PMTs have been validated, especially to ensure a linear response up to very large signals [16].

The SSD acquisition is performed in slave mode, *i.e.*, only when triggered by the associated WCD. The dynamic range of measurement must span from the signal of a single particle, mandatory for calibration purposes, to more than 10^4 MIP to be consistent with the WCD extended dynamic range (see sect. **2˙2**). For this reason, the anode signal of the SSD PMT is split into two different channels, the first one amplified 32 times and the other attenuated by a factor of 4.

The combination of the SSD and WCD measurements will allow to disentangle the muonic and electromagnetic components of the showers by exploiting the different responses of the two detectors. In fact, muons have larger energy deposits in water than electromagnetic ($e^-/e^+/\gamma$) particles; instead, both deposit on average the same amount of energy in the scintillator. In this sense, a WCD is more sensitive to muons, whereas a SSD to the electromagnetic part of shower.

2˙2. *The Small PMT (SPMT).* – A limiting factor in the current measurements of the WCDs is the saturation of the signals in stations near the impact point of the shower core (that is the central region of the cascade) at the ground, where the particle density dramatically increases. Such issue affects more than 30% of the events above $\sim 10^{19.5}$ eV, thus reducing the precision of any reconstruction method at the highest energies. To extend the dynamic range of unsaturated signal acquisition [17] an 1-inch Hamamatsu R8619 photomultiplier tube is added to each WCD, exploiting an unused 30 mm window on the Tyvek bag containing the ultra-pure water. The SPMT features the same bialkali

photocathode of the standard WCD 9-inch PMTs, but with an active area ∼80 times smaller. Adjusting its gain, signals can be collected as close as 250–300 m from the shower core without saturation, broadening the WCD dynamic range by more than a decade (up to 20,000 VEM) and thus allowing to record events above 10^{20} eV unambiguously, *i.e.*, with complete signals in all stations.

The SPMT was designed with a passive base, moving the power supply into a separate module, a custom-made CAEN-A7501 HV DC-DC converter hosted in a metallic box. This allows to minimize the number of failures and to ease the maintenance with respect to the standard WCD 9-inch PMTs, which are instead supplied through an active base soldered to the PMT leads and insulated by silicon potting.

All the SPMTs [14] and the HV power supply modules [18] have been tested and sent to the Pierre Auger Observatory site, and are deployed together with the SSD PMTs and the upgraded electronics.

2˙3. *The Radio Detector array (RD).* – The RD [19] consists of an array of 1.2 m diameter short aperiodic loaded loop antennas (SALLA) collecting the radio emission from air showers along two orthogonal polarization directions, in the frequency range 30–80 MHz. The SALLA fulfills the need for both ultra-wide band sensitivity (flat function of radio frequency) and low costs for production and maintenance, as required for a large-scale radio array. Moreover, by design, the reception from below is strongly suppressed to make the antenna almost insensitive to the underlying structures and ground conditions, since each unit is mounted on top of a WCD. The signals are processed by a dedicated electronics board, operating in slave-trigger mode. All the components of the upgraded SD station have been carefully optimised to ensure minimal electromagnetic interference in the relevant frequency band.

The radio emission of extensive air showers mainly arises from the geomagnetic deflection of the electrons and positrons in opposite direction, and secondarily due to the time variation of the electron excess along the longitudinal development of the shower (Askaryan effect). The RD is therefore sensitive to the electromagnetic component of the EAS and will complement the information obtained from the SSD+WCD system [20] especially for inclined showers, where the electromagnetic particles are largely absorbed and only the muonic component reaches the WCD. As it is negligibly absorbed in atmosphere, the radio emission depends only on the source distance and not on the amount of traversed matter.

The feasibility of radio detection of EAS using a grid of antennas with 1500 m spacing was predicted by simulations and demonstrated effective for inclined events (zenith angle of the shower larger than 65°) by the AERA results [21]. The footprint of detectable radio signals at the ground level was found to cover areas of the order of tens of km^2 in size, increasing with the inclination of the shower axis.

2˙4. *The Underground Muon Detector (UMD).* – The UMD [22] consists of an array of buried scintillators associated with the 73 WCDs of the two denser arrays with spacing 750 m and 433 m deployed in the north-western part of the Observatory. At each position three 10 m^2 modules are installed 2.3 m underground (bottom right part of fig. 1). Each module is composed of 64 scintillator strips (4 m × 4.1 cm × 1 cm) coupled to wavelength-shifting optical fibres read by an array of Hamamatsu S13361-2050 silicon photomultipliers (SiPMs). While the trigger is provided by the associated WCD, a dedicated UMD electronics performs the acquisition simultaneously in two different modes: by processing separately the 64 binary traces from each strip (*binary acquisition mode*)

to count single muons; by summing analogically the 64 SiPM signals (*ADC mode*) to estimate the density of muons when the binary mode is saturated.

Since the electromagnetic component of the showers is largely absorbed before reaching the UMD modules, these detectors allow a direct measurement of the muonic component [23, 24], an invaluable information to cross-check and fine-tune the analysis method employing the combined observations from the AugerPrime detectors. Additionally, the UMD measurements will greatly enhance the studies of hadronic interactions and of the primary composition in the lower energy range, corresponding to the transition from Galactic to extra-galactic cosmic rays.

2˙5. *The Upgraded Unified Electronics (UUB).* – The UUB [25] consists of a single board which processes the signals of the four WCD PMTs plus the SSD PMT and accomplishes their calibration, generates the local WCD triggers, interfaces with the UMD and RD systems, provides the GPS time tagging and handles the communication to the Central Data Acquisition System via radio transmission. It was designed to fit the old electronics enclosure and to accept the existing WCD-PMTs, GPS antenna, communication and power supply cables. However, with respect to the old electronics, the UUB features: faster flash ADCs (from 40 to 120 MHz); increased resolution of the dynamic range (from 10 to 12 bits); significantly more powerful FPGA and 10 times faster CPU; improved timing accuracy (down to ≈2 ns). The data with the original 120 MHz sampling rate are transmitted and employed in the actual analyses and reconstruction. The backward compatibility with the previous acquisition is currently maintained by digitally filtering and down-sampling the measured signal traces to emulate current triggers.

Before delivery to the experimental site, the boards were tested by the manufacturer (A4F company, previously SITAEL SpA) after production, and then underwent an Environmental Stress Screening tests [26] performed in Prague by the local Collaboration group.

3. – Current status

A pre-production array of 77 SSDs was deployed in March 2019, adapting the setup to the old electronics. The results demonstrated a very good stability in the SSDs performances, as shown in the left side of fig. 2, where the vertical patterns signal the occurrence of thunderstorms (darker color) or temporary communication default in the array (in grey). Moreover, the difference in the baseline fluctuations between night and daytime has been found to be highly compatible over the whole period, confirming the light tightness of the SSD units [13].

Starting from the end of 2020, an increasing part of the SD array has been upgraded with the installation of the UUBs together with the SPMTs and SSD PMTs. The upgraded stations are operating well within the design requirements and the collected data allows to study the WCD (with SPMT) and SSD acquisition. The signals of the 9-inch WCD PMTs are measured in units of the signal produced by a vertical muon traversing the tank at its center (Vertical Equivalent Muon, VEM), while the SSD calibration is based on the charge of a minimum-ionizing particle (MIP). Both the calibration procedures are performed by using background muons, and about 40% of the WCD VEM calibration triggers produce a MIP in the SSD. Instead, due to its small area, the SPMT cannot be calibrated using atmospheric muons. A dedicated selection of signals from small local shower has been set up to cross-calibrate the SPMT using the VEM-calibrated signals of the 3 other WCD PMTs. In the right panel of fig. 2, the correlation between

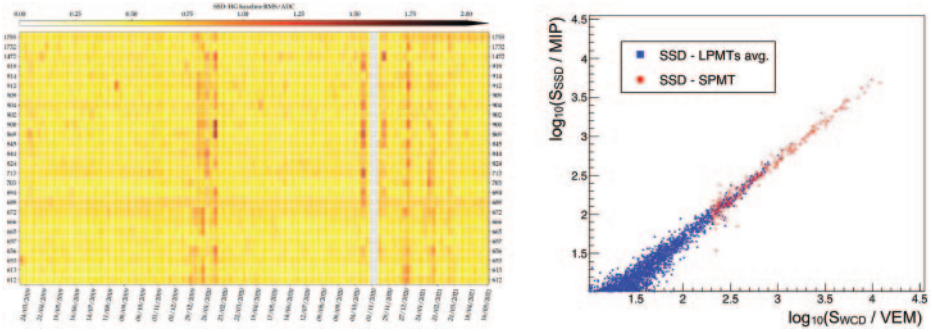

Fig. 2. – Left: evolution of the RMS in ADC counts for the PMTs trace of a subsample of preproduction SSDs. Right: SSD *vs.* WCD integrated signals. The 9-inch WCD-PMTs signals (blue dots) are used up to the saturation; the measurements are extended up to ∼20000 VEM by means of the SPMT (red dots). Plots from ref. [13].

signals from EAS events, collected in about two months of data-taking, demonstrates that the measurements are successfully accomplished up to the highest particle densities. In particular, the dynamic ranges of the WCD and SSD clearly match, as required in order to benefit the most from the combined detection of the showers.

A RD engineering array of 10 prototype SALLAs, of which 7 in acquisition in a complete hexagon, has been installed in November 2019. The in-situ calibration is based on the comparison of the frequency and time-dependent background power received from the sky with the predicted Galactic radio emission. An end-to-end pilot calibration procedure has been developed and presented in ref. [27], confirming the feasibility of an absolute energy calibration of the full RD array (see for example ref. [28]).

A total of 31 UMD positions have been already deployed, of which 26 in acquisition. The collected data show a good long-term stability in the monitored parameters [29], in particular confirming the efficiency in the temperature compensation mechanism employed to maintain a uniform gain among the SiPMs of the whole UMD array. Moreover, a dedicated procedure for the calibration of the two acquisition modes (binary and ADC) has been finalized [30].

3˙1. *Deployment and commissioning.* – The installation of the SSD units has been completed in March 2022 (except for two inaccessible areas in the north-east and west of the array). More than half of the SD array (around 850 stations) has been equipped with UUB, SSD PMT and SPMT at the moment of writing. The upgrade of the SD stations (excluding for the moment the RD antennas) is envisaged to be completed by mid-2023.

The assembly, deployment and commissioning of the UMD array is also currently underway, while the installation of a first batch of RD antennas is planned for the first quarter of 2023, with the deployment of the full array scheduled to be completed by the end of the same year.

4. – Expected performances

As previously discussed, the upgrade will increase the Pierre Auger Observatory sensitivity to the mass of UHECRs, in particular in the energy range of the flux suppression, with the goal of discriminating between different astrophysical scenarios. To evaluate

the AugerPrime physical reach, two different benchmark models have been assumed, that reproduce (within the uncertainties) the energy spectrum and $X_{\rm max}$ distributions as currently measured above $10^{18.7}$ eV:

- a maximum rigidity model (*scenario 1*), where the sources are assumed to accelerate the primaries up to a maximum energy proportional to their charge number Z. In this scenario, the flux suppression is caused by the cutoff of the spectrum at the sources and the composition becomes heavier for increasing energies, with a proton component dominating around $10^{18.5}$ eV and heavy elements of the iron group at the upper end;

- a photo-disintegration model (*scenario 2*) where the sources accelerate the primaries above the energy threshold for the photo-disintegration on CMB photons, meaning that the lighter particles reaching Earth can be originated from the fragmentation of the original nuclei. In this scenario the flux suppression is caused by the energy loss processes during propagation and only a negligible fraction of light elements could be accelerated in the sources to describe the Auger data.

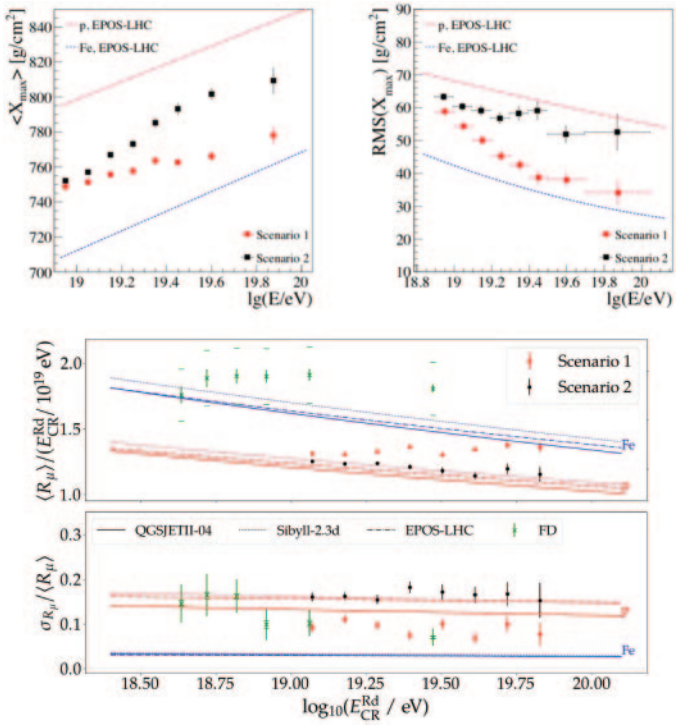

Fig. 3. – Upper plots: mean depth of shower maximum $X_{\rm max}$ (left) and its fluctuations (right) evaluated for the two scenarios (1 = maximum rigidity; 2 = photo-disintegration) using 7 years of simulated WCD+SSD data only. Plots from ref. [11]. Bottom plots: mean muon number (top) and fluctuations in the number of muons (bottom) obtained for the two different scenarios simulating 10 years of combined RD + WCD measurements. In green, the current results from the hybrid (SD + FD) dataset. Plots from ref. [20].

Two set of mock events (with zenith below 60°) corresponding to 7 years of data-taking have been simulated to study the first two moments of the $X_{\rm max}$ distributions obtained using the WCD + SSD measurements. The results are reported in the left part of fig. 3, where the expectations for pure proton and pure iron compositions are also illustrated for reference. While the predictions for the two models are similar below $10^{19.2}$ eV (the range currently reached with enough statistics by the FD measurements) they differ in the highest energy region, confirming that the two scenarios can be distinguished with high significance within 7 years of data-taking.

To demonstrate the potential of RD+SD hybrid measurements in the determination of the UHECR composition, the relative number of muons $\langle R_\mu \rangle / (E_{\rm CR}/10\ {\rm EeV})$ and its physical fluctuations $\sigma_{R_\mu}/\langle R_\mu \rangle$ (estimated by subtracting the detector and energy resolutions) have been studied using a mock dataset of inclined air showers (zenith above 60°) simulated according to the two benchmark models. As can be seen in the bottom panel of fig. 3, with the statistics expected for the RD in 10 years of data-taking (more than one order of magnitude larger than the FD one at energies above 10^{19} eV) the difference between the two scenarios appears again highly significant, especially considering the physical fluctuations which are much less affected by the systematic uncertainty in the energy scale (error caps of the green data points, see full explanation in ref. [20] and references therein).

5. – Conclusions and outlook

The AugerPrime upgrade of the Pierre Auger Observatory will substantially enhance the sensitivity to the mass composition of primary cosmic rays, especially in the region of the flux suppression (namely above 4×10^{19} eV). This goal will be achieved by measuring extensive air showers using simultaneously water-Cherenkov, scintillator and radio detectors and underground muon counters, as shown in the spectacular multi-hybrid event in fig. 4, and with a nearly 100% duty cycle (compared to the ∼15% duty cycle of the standard hybrid WCD + FD measurements). The information about the primary UHECR mass will be obtained through the separation of the muonic and electromagnetic components on an event-by-event basis, comparing the SSD and WCD signals in *vertical* showers (arrival direction $\theta < 60°$) and exploiting the combination of RD and WCD

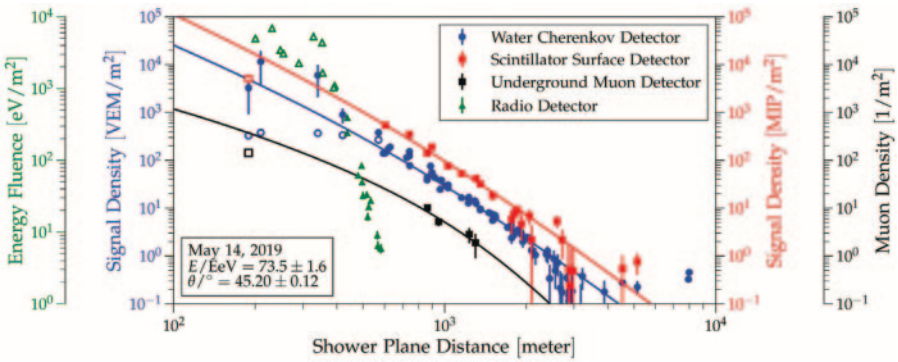

Fig. 4. – Signal densities, as a function of the distance to the shower core, for a real event measured with WCDs (blue), pre-production SSDs (red), UMDs (black) and RD antennas (green).

observations for *inclined* ones ($\theta > 60^\circ$).

The results are expected to greatly improve our understanding of the candidate sources and of the origin of the flux suppression of UHECR, while also allowing the study of high-energy neutrino and γ-ray fluxes and the search for a possible proton contribution at the highest energies. Moreover, the augmented measurements will provide superior data to improve the present hadronic interaction models and possibly solve the inconsistencies in the muon-content prediction with simulated showers.

The deployment and commissioning of AugerPrime are planned to be completed by 2023, while the data-taking is foreseen to continue up to the beginning of the next decade, representing a fundamental input for future experiments in the field.

* * *

The successful installation, commissioning and operation of the Pierre Auger Observatory and of the AugerPrime upgrade would not have been possible without the strong commitment and effort from the technical and administrative staff in Malargüe, and the financial support from a number of funding agencies from the participating countries, listed at `https://www.auger.org/collaboration/funding-agencies`.

REFERENCES

[1] Aab A. *et al.*, *Nucl. Instrum. Methods A*, **798** (2015) 172.
[2] Novotný V., *PoS(ICRC2021)*, **395** (2021) 324.
[3] Aab A. *et al.*, *Phys. Rev. Lett.*, **125** (2020) 121106.
[4] Yushkov A., *PoS(ICRC2019)*, **358** (2019) 482.
[5] Todero Peixoto C. J., *PoS(ICRC2019)*, **358** (2019) 440.
[6] Aab A. *et al.*, *Science*, **357** (2017) 1266.
[7] de Almeida R., *PoS(ICRC2021)*, **395** (2021) 335.
[8] Aab A. *et al.*, *Astrophys. J.*, **935** (2022) 170.
[9] Biteau J., *PoS(ICRC2021)*, **395** (2021) 307.
[10] Aab A. *et al.*, arXiv: 1604.03637 [astro-ph.IM].
[11] Castellina A., *EPJ Web of Conferences*, **210** (2019) 06002.
[12] Soldin D., *PoS(ICRC2021)*, **395** (2021) 349.
[13] Cataldi G., *PoS(ICRC2021)*, **395** (2021) 251.
[14] Pekala J., *PoS(ICRC2019)*, **358** (2019) 380.
[15] Taboada A., *EPJ Web of Conferences*, **210** (2019) 02016.
[16] Buscemi M. *et al.*, *JINST*, **15** (2020) P07011.
[17] Castellina A., *PoS(ICRC2017)*, **301** (2017) 397.
[18] Anastasi G. A. *et al.*, *JINST*, **17** (2022) T04003.
[19] Pont B., *PoS(ICRC2019)*, **358** (2019) 395.
[20] Schluter F., *PoS(ICRC2021)*, **395** (2021) 262.
[21] Aab A. *et al.*, *JCAP*, **10** (2018) 026.
[22] Botti A. M., *PoS(ICRC2019)*, **358** (2019) 202.
[23] Aab A. *et al.*, *Eur. Phys. J. C*, **80** (2020) 751.
[24] Aab A. *et al.*, *Phys. Rev. Lett.*, **126** (2021) 152002.
[25] Marsella G., *PoS(ICRC2021)*, **395** (2021) 230.
[26] Bohacova M., *PoS(ICRC2019)*, **358** (2019) 199.
[27] Fodran T., *PoS(ICRC2021)*, **395** (2021) 270.
[28] Aab A. *et al.*, *Phys. Rev. Lett.*, **116** (2016) 241101.
[29] Botti A. M., *PoS(ICRC2021)*, **395** (2021) 233.
[30] Aab A. *et al.*, *JINST*, **16** (2021) P04003.